# Design and analysis of the performance of multi-source interconnected electrical power system using resilience random variance reduction technique

**B. PRAKASH AYYAPPAN**[1]* **and R. KANIMOZHI**[2]

[1] Department of Electrical and Electronics Engineering, V.S.B Engineering College, Karur and Research Scholar (Electrical), Anna University, Chennai, Tamilnadu, India

[2] Department of Electrical and Electronics Engineering, University College of Engineering, Anna University-BIT Campus, Tiruchirapalli, Tamilnadu, India

**Abstract.** The increasing demand for electricity and global attention to the environment has led energy planners and developers to explore developing control techniques for energy stability. The primary objective function of this research in an interconnected electrical power system to increase the stability of the system with the proposed RRVR technique is evaluated in terms of the different constraints like THD (%), steady-state error (%), settling time (s), overshoot (%), efficiency (%) and to maintain the frequency at a predetermined value, and controlling the change of the power flow of control between the areas renewable energy generation (solar, wind, and fuel cell with battery management system) based intelligent grid system. To provide high-quality, reliable and stable electrical power, the designed controller should perform satisfactorily, that is, suppress the deviation of the load frequency. The performance of linear controllers on non-linear power systems has not yet been found to be effective in overcoming this problem. In this work, a fractional high-order differential feedback controller (FHODFC) is proposed for the LFC problems in a multi-area power system. The gains of FHODFC are best adjusted by resilience random variance reduction technique (RRVR) designed to minimize the overall weighted absolute error performance exponential time. Therefore, the controller circuit automatically adjusts the duty cycle value to obtain a desired constant output voltage value, despite all the grid system's source voltage and load output changes. The proposed interconnected multi-generation energy generation topology is established in MATLAB 2017b software.

**Key words:** multi-source and single-area interconnected power system; LFC; resilience random variance reduction technique.

## 1. INTRODUCTION

For the power system's reliable and stable operation, the system should be maintained at a predetermined frequency value or adjust the deviation in the load demand and supply is changed with less time. The total power of the power system is used to provide steady-state load conditions. Sudden and random changes in load demand cause sudden and random changes in load and power generation. This situation leads to changes in generator speed, which directly affects the frequency of the system. Therefore, the control system must be zero to solve this problem by forcing the two mismatches and a tie-line power system frequency error. The load frequency control maintains the power flow in a contact line at a predetermined value and a standard system frequency and interference conditions. This work proposes a structure of a modification of the fractional high-order differential feedback controller and two similar design field generating diverse sources, including solar / wind and the fuel cell system AGC implementation. The controller's parameters are optimized with the so-called resilient random

variance reduction technology, a recently developed heuristic technology inspired by nature. The proposed stability has been tested in three different scenarios in multi-source power units in two areas.

In this operation, the series compensator real power is injected into the system while reducing the voltage drop. The fractional high-order differential feedback controller produces appropriate feedback to the system and improves the system's power quality. In this situation, the minimum actual power is injected to reach the rated load voltage in the grid system to maintain the active power operation. All these operations are performed at the fundamental positive sequence voltage. Based on the realized resilience random variance reduction technique, the following parameters are based on the proposed converter circuit optimization: proper optimization of reduced harmonic distortion, improved steady-state, and efficiency. Power quality in electric networks is one of today's most concerning areas of the electric power system. The power quality has profound economic implications for consumers, utilities and electrical equipment manufacturers. In simpler words, power quality, electrical boundaries allow a piece of equipment to function in its intended manner without significant performance loss or life expectancy. This definition embraces two things that we demand from an electrical device, namely performance and life

B. Prakash Ayyappan and R. Kanimozhi

expectancy. Photovoltaic systems will witness continuous and will contribute significantly to electricity production for households and buildings in general. Terrestrial applications of photovoltaic panels provide auxiliary means of power generation. Although its penetration is limited because of its high capital cost and low efficiency, ongoing research is continuously weakening these barriers, increasing the use of PV electrical sources. Research on distributed electrical resources connected to the grid is the central issue for installing mega watts of PV farms and increasing its use. Continuously monitoring these installations is a very important matter because it gives feedback on improving the connectivity performance, how to increase the production and how to optimize control strategies.

Although utilities have made many efforts, some consumers require a level of PQ higher than the level provided by modern electric networks. This implies that some measures must be taken in order to achieve higher levels of power quality. It is used to define various types of disturbances to the average power system voltage. Various disturbances such as harmonics, transients, outages, faults, sags, swells, dips and flickers can be associated with the power quality. Total harmonic distortion, or THD, is the summation of all harmonic components of the voltage or current waveform compared against the fundamental component of the voltage or current. The result is a percentage of harmonic components to the fundamental component of a signal. The higher the percentage, the more the distortion that is present on the mains signal. PI controller will not increase the speed of response. It can be expected since the PI controller does not have the means to predict what will happen with the error in the near future. This problem can be solved by introducing RRVR, which can predict what will happen with the error shortly and thus decrease the controller's reaction time compared with existing controllers, and the system's efficiency is improved.

## 2. LITERATURE SURVEY

Multi-source and multi-area systems must identify the shortcomings of the conventional methods given below to improve the proposed system's stability. The LFC is a basic process in which the power system is interconnected. This system is specially designed to improve power quality with fewer harmonics distortions within this range; in this research, high order and fractional order are developed to suit LFC problems in multi-region power systems [1]. The energy management of a multi-micro grid (MMG) system is a complex problem: the coordinate distribution of the individual MG, the power exchange of the MG, and the generation unit in the power transaction between the grid and the MG [2]. The main idea of this framework applies to reality and large power systems. It has been used in the comparative balance using historical data to provide a new strategy, the strategic goal of providing support [3–5].

However, in a multi-regional area, the electric power system is the key to evaluating trade-offs and providing an adequate supply of the transmission, storage, and synergy RES. In this work, we propose a new method to quantify renewable energy sources (RES) and storage capacity credit (CC) multi-area power

systems [6]. A new power system control method has recently been proposed. To maintain economic operation, combined economic dispatch (ED) and automatic power generation control (AGC), when the power generation meets the problems of both demand and high penetration of renewable energy [7–10]. The above research on the dispatched power flow among the distributed energy management system (DEMS) is utilized to manage the network equivalent data to the transmission system concerned [11]. The goal is to diminish the total system cost in the planning cycle, including investment and operating costs, maintain the residual value, and withstand the system's short-term operation reliability and long-term restraint. The multi-zone expansion planning problem is broken down into planning problems and annual reliability sub-problems [12–16]. A coordination droop control strategy can provide a frequency region through a transmission AC grid integrated wind farm.

However, such a strategy inevitably leads to DC offset exchanging information transmission frequency region, thereby deteriorating stability and safety multi-area transmission system operation [17]. The data control area's optimal scheduling is achieved, including store operations, to achieve congestion relief. The distributed approach retains the responsibility of the control area [18–21]. moth flame optimization (MFO) is one of the latest optimization algorithms used for hydraulic, thermal, and natural gas hybrid power generating sets; in this article, it is used to find PID controllers' best parameters for AGC system [22–24]. Due to the discontinuity and haphazardness of sun-powered and wind vitality, it has a dangerous effect on the grid in the grid-connected mode of operation, and at more situational conditions, the yield of PV and wind power generation gives oscillation. The reactive power-sharing has been formulated and correctly performed to compensate for a voltage drop of the line. Exacting tracking performance can be attained by rational tuning the system parameters [25]. The simulations results of the protections during faults in the grid nodes are different for each protection system [26]. The parameters are determined based on the data for steady and transient states simulations in a power system [27]. In distributed generation systems, power electronic converters are applied as interfaces for matching parameters of distributed sources with power lines and coupling energy storage with power lines [28]. The proposed method gives robust performance against the disturbance in loading conditions, variation of system parameters. The simulation outcomes showed a good dynamic performance of the proposed controller [29]. This article demonstrates multi-area power systems' resilient event-triggered load frequency control under non-ideal network environments to preserve the desired control performance and improve communication efficiency [30]. In general, the potential energy futures are a simple function of the technologies utilized, but they will also be shaped by the social relations that configure societies [31].

## 3. PROPOSED SYSTEM

In principle, UPQC is an integrated shunt and a series of active power filters with a common self-sustaining DC bus. Figure 1 shows the proposed renewable source interconnected with the

**Fig. 1.** Proposed block diagram using resilience random variance reduction technique



**Fig. 2.** Equivalent circuit of solar cell

shunt resistance $R_{sh}$ is usually less than a shunt resistor. Finally, the generated $V_{\text{PV}}$ voltage determines the single-cell voltage. The actual physical equivalent circuit of a photovoltaic cell is shown in Fig. 1.

Figure 2 clearly shows that current $I$ passes through the load as follows:

$$I = I_{ph} - I_d - I_{sh}$$
$$= I_{ph} - I_0 \left( e^{q\left(V_{\text{PV}} + \frac{IR_s}{AkT}\right)} - 1 \right) - \frac{V_{\text{PV}} + IR_s}{R_{sh}}, \qquad (1)$$

where $I$ is the output current of the PV cell. $I_{ph}$ is an electric current generated by sunlight. Also, $I_d$ passes through the diode's P-N junction, also known as the dark current's leakage current. $I_{sh}$ is bypass current. $I_0$ is the reverse saturation current of the diode. q is the electronic power $(1.6 \times 10^{19} °\text{C})$. $V_{\text{PV}}$ is the output voltage of the photovoltaic cell. $R_s$ is the resistance of a series of photovoltaic cells. A is the factor of the diode and its value is $1 \sim 2$. In the equation, $k$ is Boltzmann's constant $(1.38 \times 10^{-23} \text{ J/K})$; similarly, $T$ is the absolute temperature. $R_{sh}$ is the parallel resistance of the photovoltaic cell. Under ideal mode conditions, $R_{sh}$ can be ignored. In this state $I$ passes through the load as expressed below:

$$I = I_{ph} - I_d = I_{ph} - I_0 \left( e^{q\left(V_{\text{PV}} + \frac{IR_s}{AkT}\right)} - 1 \right). \qquad (2)$$

The single diode-based solar power generation is described above. The series and parallel combination of the PV array solar power generation is used for high voltage generation purposes.

### 3.2. Wind power
The power generated from a wind turbine is subjective by several factors, including turbine size, wind direction, turbine position, wind speed, and the dynamic performance and load distribution of parallel turbine generators. In order to generate electricity in the wind farm in independent mode, permanent magnet synchronous machines are used. They are mechanically connected to the wind turbine. The mechanical power generation of the wind turbine depends upon wind speed, and the power output relative to the pitch angle of the wind turbine is given as:

$$P_{\text{mech}} = \frac{8}{27} \rho V^3 A. \qquad (3)$$

where: $\rho$ is air density, $V$ is wind speed, $A$ is sweep area of the rotor.

UPQC model. The proposed resilience random variance reduction technique will analyze the source power and load power and maintain the power stability using the UPQC compensator. The transmission of power from renewable energy sources to multiple power sources must use RRVR technology to solve power quality issues for proper management. Accordingly, the system is designed to prevent loss of power and over-voltage and under-voltage operation so that the grid can operate normally. The power management system is efficiently optimized using a converter with resilience random variance reduction technique (RRVR). Finally, the stabilized DC output is given to the grid converter for the grid-connected application. The RRVR controller's benefits will spontaneously adjust the duty cycle value to obtain a desired constant output voltage value, despite all the source voltage and load output changes. The new topology assimilates multiple renewable energy and powers multiple loads with changed output levels.

### 3.1. Solar power generation
When the PV cell's energy generation is based on the irradiation by the sun, $I_{Ph}$ source current passes through the diode $I_d$. If there is any leakage, it is determined by dark current. In these equivalents, circuit series resistance $R_s$ and parallel resistance $R_{sh}$ are included. The main purpose of the series resistance $R_s$ forms the diffusion resistance level, greater than $1 \Omega$. The
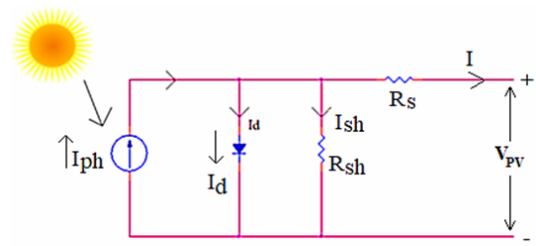
Bull. Pol. Acad. Sci. Tech. Sci. 69(5) 2021, e137941

3

The pitch angle controls the rotor's sweep area; the turbine's mechanical power is fed to the rotor of the DFIG (double-fed induction generator) mechanically coupled by the shaft. The three-phase AC output of DFIG is fed to a rectifier controlled by a diode bridge rectifier and a DC-DC converter. The output voltage of the controlled rectifier can be controlled by changing the duty cycle of the pulse. The reference is controlled and changed to the converter's reference value through a feedback loop with the DC link voltage. The internal model of the wind farm can be seen below in Fig. 3.

**Fig. 4.** Equivalent circuit of fuel cell

**Fig. 3.** Block for wind energy system

A relative power-controlled DC–DC converter controlled by the feedback voltage direction is used. Three power electronic switches (MOSFETs) are connected to the three-phase diode bridge rectifier to convert 3-phase AC into variable DC. The DC variable DC fixed voltage ripple generated by the control of the DC–DC converter is reduced. A dynamic duty cycle of MOSFET and the switching frequency is 45 kHz. The passive components of the DC–DC converter are calculated and given below. L is the input inductance and is given as;

$$L = \frac{D \cdot V_{in}}{F_s \cdot \Delta iL}. \tag{4}$$

$V_{in}$ is the input voltage of the converter, $F_s$ is the switching frequency of the converter, and $iL$ is a current flowing in the inductor. The output capacitance of the capacitor $C$ is calculated as:

$$C = \frac{I_{dc}}{2 \cdot W \cdot \Delta V_{dc}}. \tag{5}$$

The directional voltage feedback loop controls the DC–DC converter's output to control the conduction time of the MOSFET. The controller generates a relatively high-frequency triangular wave to generate the duty cycle of the pulse fed to the MOSFET. Finally, the stabilized voltage is supplied to the grid converter, the DC–AC converter, and the grid-connected operation.

### 3.3. Fuel cell energy generation
In the introduction of fuel cell and DC–DC converter, an effective mode is shown in Fig. 4, and the circuit includes a fuel cell generator, a boost DC–DC converter and a load. In the step-up DC–DC converter, the load's output voltage can be adjusted
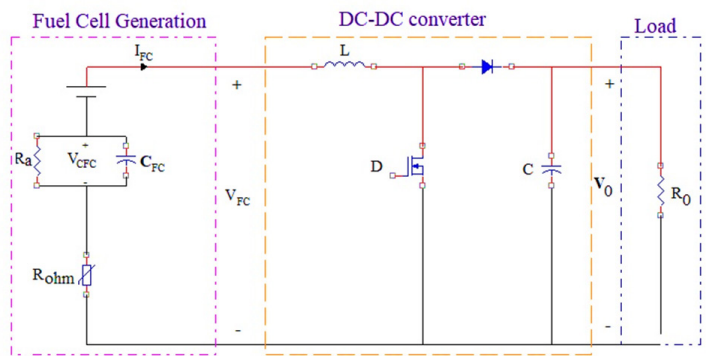
to the required voltage. The output voltage can be controlled by the variable duty cycle (d) of the boost DC–DC converter.

The circuit of Fig. 4 in this system can be analyzed based on the boost converter's switching state. When the switch is closed, the diode is reverse biased. Figure 5 shows the equivalent circuit of the system when the switch is closed. Including the fuel cell, the path around the inductor and the closed switch, Kirchhoff's voltage law is

$$V_L = V_{FC}. \tag{6}$$

When the switch is opened, the inductor current cannot change immediately, and the diode becomes forward biased to provide a path for the inductor current. Figure 6 shows the equivalent circuit of the system when the switch is turned on. Assuming a constant output voltage $V_0$, the voltage across the inductor is
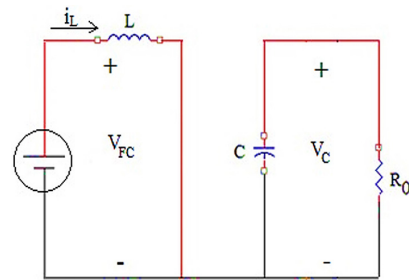
$$V_L = V_{in} - V_0. \tag{7}$$

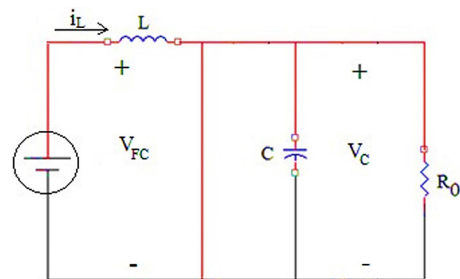**Fig. 5.** Equivalent circuit when the circuit switch is open

**Fig. 6.** Equivalent circuit when the circuit switch is closed

4

Bull. Pol. Acad. Sci. Tech. Sci. 69(5) 2021, e137941

www.czasopisma.pan.pl    PAN    www.journals.pan.pl
POLSKA AKADEMIA NAUK

Design and analysis of the performance of multi-source interconnected electrical power system using resilience random variance reduction technique
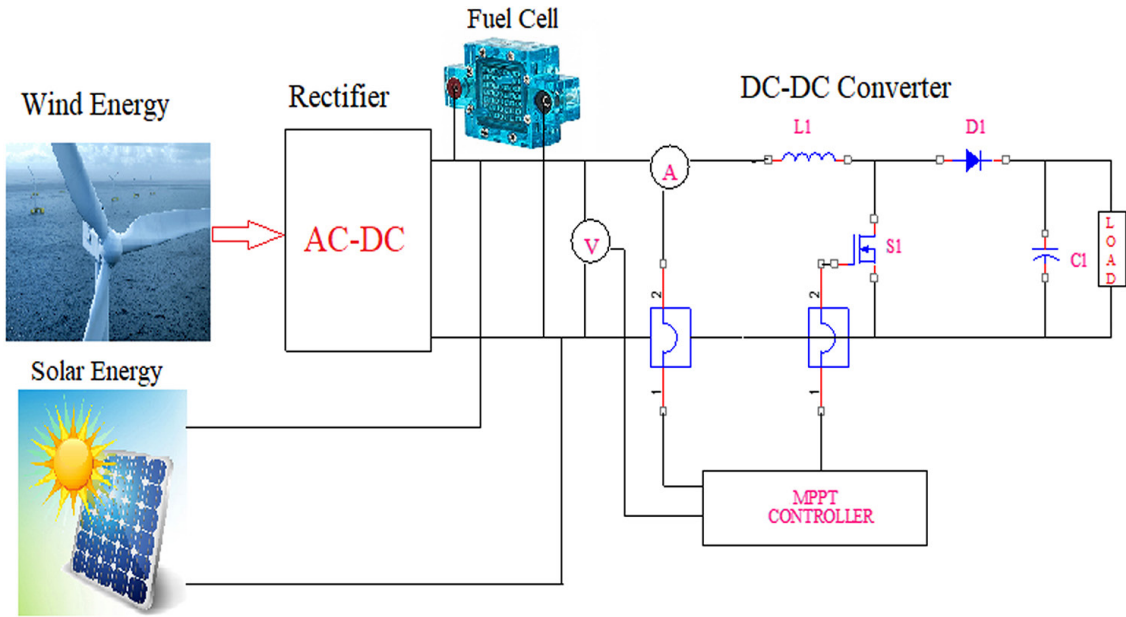
**Fig. 7.** Wind-based MPPT system

For periodic operation, the average inductor voltage must be zero. The average inductor voltage expressed in a switching cycle is

$$V_L = D(V_{in}) - (1-D)(V_{in} - V_0) = 0. \tag{8}$$

Solving for

$$V_0 = \frac{V_{in}}{1-D}. \tag{9}$$

The normal duty cycle, d, is defined as the switch time, the total switching period. From (9) in steady-state, the gain ratio between the output and the input can be verified by the following expressions,

$$M = \frac{V_0}{V_{in}} = \frac{1}{1-D}. \tag{10}$$

### 3.4. Resilience random variance reduction technique (RRVR) based MPPT system

The operating point of PV, wind, and fuel cells depends on the maximum extractable power strength. The improved power generation using the DC–DC converter is shown in Fig. 7.

The MPPT concept enhances the power generation for renewable energy generation. The MPPT is designed to obtain MPP from the PV, wind and fuel cell and optimize the generation voltage using a DC–DC converter.

#### 3.4.1. Resilience random variance reduction technique (RRVR) MPPT

An RRVR–MPPT technology is applied to track the solar, wind, and fuel cell system's optimal operating point. In this technical state, the power slope is empty, positive and negative, respec-

tively, in MPPT (DP/DV = 0), left MPPT and right MPPT. Due to this fact, MPPT can be found in terms of;

$$P_{pv} = P_{pv} \times i_{pv}, \tag{11}$$

$$\frac{\partial P_{pv}}{\partial V_{pv}} = i_{pv} + v_{pv} \times \partial i_{pv/\partial v_{pv}} = 0, \tag{12}$$

$$\partial i_{pv/\partial v_{pv}} = -i_{pv/v_{pv}} \quad \text{at MPP}, \tag{13}$$

$$\partial i_{pv/\partial v_{pv}} > -i_{pv/v_{pv}} \quad \text{at the left of MPP}, \tag{14}$$

$$\partial i_{pv/\partial v_{pv}} < -i_{pv/v_{pv}} \quad \text{at the right of MPP}. \tag{15}$$

### 3.5. Bi-directional converter-based battery management

The battery-based charging system is shown in Fig. 8. This converter circuit's proposed bidirectional converter (BDC) circuit diagram consists of an input capacitor $C_2$ and MOSFET switches $S_2$ and $S_3$ and output inductor $L_2$, and capacitor $C_3$
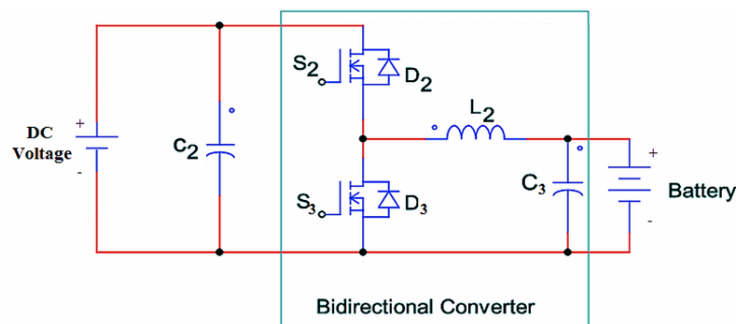


**Fig. 8.** Bi-directional battery-based battery management

Bull. Pol. Acad. Sci. Tech. Sci. 69(5) 2021, e137941

5

with battery. The diodes $D_2$ and $D_3$ are anti-parallel body diodes of the power MOSFETs $S_2$ and $S_3$.

$$C_{bat}(t) = C_{bat}(t-1) \cdot (1-\sigma)$$
$$+ \left[ \text{BESS}_S(t) + E_w(t) - \frac{E_L(t)}{\eta_{inv}} \right] \cdot \eta_{bat} . \quad (16)$$

When the power demand is greater than the generation, then the generation also is increased to meet the load. In this case, the battery condition wherein restriction (17),

$$C_{bat}(t) = C_{bat}(t-1) \cdot (1-\sigma)$$
$$- \left[ \frac{E_t(t)}{\eta_{inv}} - \text{BESS}_S(t) - E_w(t) \right], \quad (17)$$

where, $C_{bat}(t)$ and $C_{bat}(t)$ $(t-1)$ are the convenient capacity of battery backup $(W_h)$ concerning time $t$ and $t-1$, $\sigma$ is self-battery discharge $E_{PV}(t)$ and $E_w(t)$ are the hybrid power, $EL(t)$ is demand load time, $\eta_{inv}$ is the performance of the grid converter, $C_{bat}$ and $C_{bat}$ battery storage max and min.

If the power source's energy is sufficiently large, the excess energy charging circuit pattern is stored in the battery's operation. Otherwise, the circuit will operate in the discharge mode to provide the necessary energy to the load. Therefore, it is recommended that BDC can provide a steady and reliable power supply to the load.

### 3.6. Grid converter

The grid converter is used to convert DC to AC voltage, where the grid converter works as a single-phase or three-phase grid converter. Many grid converter models operate on single-phase or three-phase power supplies. The grid converter contains six switches, and it gives three-phase power to the grid, and the gate terminals of these six switches are connected to the controller. This resilience random variance reduction technique controller will provide suitable PWM for the grid converter switches in Fig. 9.

The grid converter has six states using resilience random variance reduction technique controller to control grid converter switches' switching. Still, they must avoid undeclared states and short-circuit conditions. Based on the variation of load voltage and current, the proposed resilience random variance reduction technique controller will vary the Pulse Width Modulation of the grid converter switches. The grid converter seven switching states are described below in Table 1.
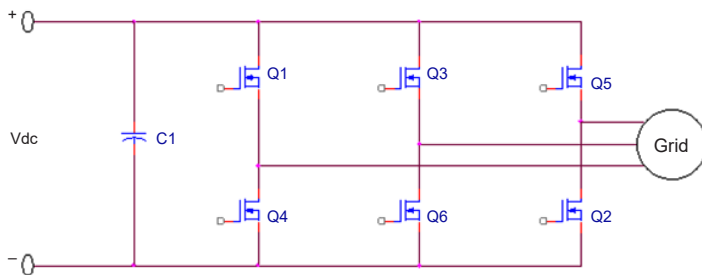


**Fig. 9.** Voltage source grid converter

**Table 1**
Switching state of the grid converter

| Switching state | $V_a$ | $V_b$ | $V_c$ |
|---|---|---|---|
| Q1–Q2–Q6 On & Q4–Q5–Q3 Off | $V_i$ | 0 | $V_i$ |
| Q2–Q3–Q1 On & Q5–Q6–Q4 Off | 0 | $V_i$ | $-V_i$ |
| Q3–Q4–Q2 On & Q6–Q1–Q5 Off | $-V_i$ | Vi | 0 |
| Q4–Q5–Q3 On & Q1–Q2–Q6 Off | $-V_i$ | 0 | $V_i$ |
| Q5–Q6–Q4 On & Q2–Q3–Q1 Off | 0 | $-V_i$ | $V_i$ |
| Q6–Q1–Q5 On & Q3–Q4–Q2 Off | $V_i$ | $-V_i$ | 0 |
| Q1–Q3–Q5 On & Q4–Q6–Q2 Off | 0 | 0 | 0 |

Grid converters use a MOSFET voltage source, such as a switch, which requires a specific gate drive signal when the VSI of the power obtained by the MOSFET used turns off their control method, and the control signal is turned on and off. The three sides with switches are used to switch Q1, Q2, Q3, Q4, Q5 and Q6. Switches Q1 and Q4, Q3 and Q6, and both sides of Q5 and Q2 cannot be operated simultaneously because of short circuits. ON and OFF from both sides of the switch are determined by RRVR technology.

### 3.7. Resilience random variance reduction technique (RRVR) for grid optimization

These works introduce the algorithm to optimize the resilience random variance reduction technique non-linear constraint in the transmission line. This technique is used to reduce power transmission loss, frequency oscillation and improve the voltage's magnitude. The gains of fractional high order differential feedback controller are employed by resilience random variance reduction technique designed to reduce the system's overall weighted absolute error performance in exponential time duration. The UPQC system can be used for the static and dynamic compensation of the ac transmission line.

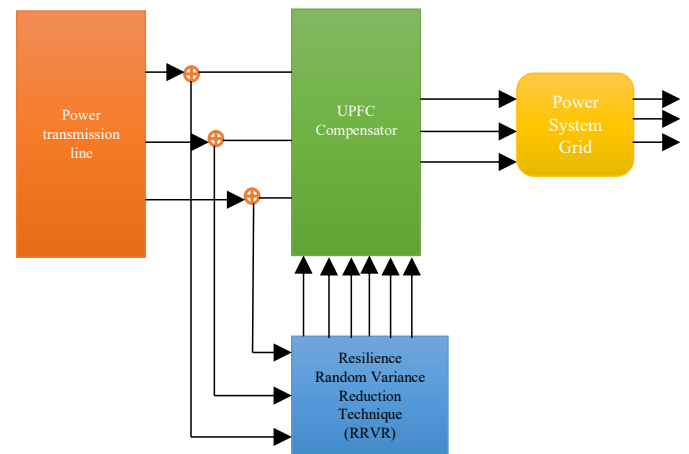Figure 10 shows the unified power quality conditioner (UPQC) based transformative power for intrinsic quality opti-



**Fig. 10.** UPQC based resilience random variance reduction technique (RRVR) for energy optimization

6

Bull. Pol. Acad. Sci. Tech. Sci. 69(5) 2021, e137941

mization algorithm presented in the transmission line. The control system describes the series and shunt converters assuming the controller's online transmission values are the fundamental components analyzed and optimized by the proposed algorithm. The determination of sudden and random changes directly affects system dynamics, and it is equally important for optimizing method performance. Sudden random variations should meet the designer's criteria, such as fast and minimal overshoot and steady-state error in response to a non-oscillating system. A more accurate system modelling or design with increased robustness and applicability of the control system is made possible through the RRVR controller in control engineering.

### 3.7.1. Resilience random variance reduction technique (RRVR)

**Inputs to the system:** The system parameters of real & reactive power flow, UPQC, oscillation in all branches.

**Outputs from the system:** Optimized VSC and real power loss
The detailed algorithm for resilience random variance reduction technique is explained in the following steps:

**Step 1:** Compute the system data such as load bus voltage values, source voltage, sag and swell voltages, and other values.

**Step 2:** Initialize the present system's value and analyze it with the resilience random variance reduction technique (RRVR).

**Step 3:** Detect the sag voltage in the transmission line and enhance the unified power flow controller using the resilience random variance reduction technique.

**Step 4:** Generate randomly 'n' number of voltage variations in grid lines. Find out the $(-V_{i\max})$ and $(+V_{i\max})$, each represents a rating sag voltage in the system.

**Step 5:** To place the all n number of voltage variation in UPQC of the respective candidate locations and load flow analysis of total real power loss $(P_L)$.

**Step 6:** Find the true power loss and use the maximum loss reduction equation to be evaluated corresponding to the number of particles per particle.

$$FV = P_{L,\text{normal}} - P_{L,\text{UPFC}}. \qquad (18)$$

**Step 7:** The change value of the obtained values and all values are the best $P_{\text{best}}$ values identified.

**Step 8:** The transformation between the maximum range in the transmission system and the average fitness value is called the error.

$$\text{Error} = (\text{maximum fitness} - \text{average fitness}). \qquad (19)$$

**Step 9:** Determine the $r_{ij}$ values of the following equation

$$r_{ij} = G_{\text{best}}FV - P_{\text{best}}FV, \qquad (20)$$

$r_{ij}$ obtained by optimizing the variance between the best fitness values $G_{\text{best}}FV$ and $P_{\text{best}}FV$

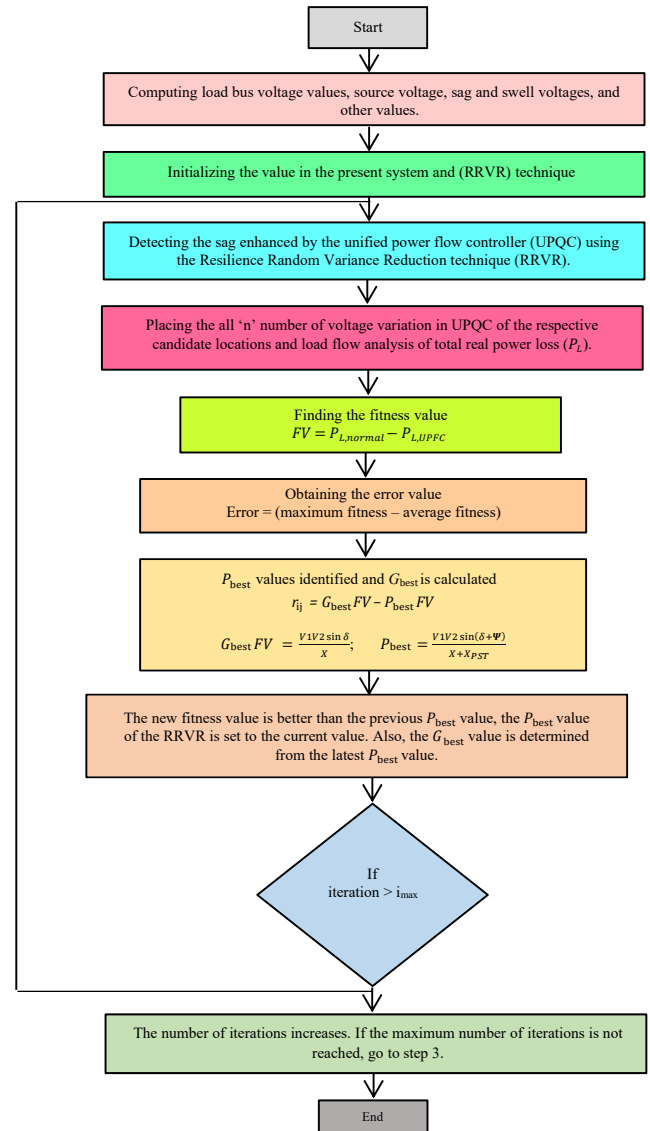$$G_{\text{best}}FV = \frac{V_1 V_2 \sin \delta}{X}, \qquad (21)$$



**Fig. 11.** Algorithm of resilience random variance reduction technique (RRVR)

where: $P$ is active power transmitted, $V_1$ is line to line voltage of source $V_1$, $V_2$ is line to line voltage $V_2$, $X$ is reactance of interactions, $\beta$ is angle of $V_1$ with respect to $V_2$.

$$P_{\text{best}} = \frac{V_1 V_2 \sin(\delta + \Psi)}{X + X_{PST}}, \qquad (22)$$

where, $X_{PST} = PST$ leakage reactance, $\Psi = PST$ phase shift angle of $T_2$ voltage with respect to $T_1$.

**Step 10:** The new fitness value calculates the new positions of all fireflies. If the new fitness value is better than the previous $P_{\text{best}}$ value, the $P_{\text{best}}$ value of the RRVR is set to the current value. Also, the $G_{\text{best}}$ value is determined from the latest $P_{\text{best}}$ value.

**Step 11:** The number of iterations increases. If the maximum number of iterations is not reached, go to step 3.

Bull. Pol. Acad. Sci. Tech. Sci. 69(5) 2021, e137941

7

B. Prakash Ayyappan and R. Kanimozhi

## 4. RESULTS AND DISCUSSION

The present modelling approach of a Mat lab-based toolbox is for developing and testing the UPQC using the algorithm resilience random variance reduction technique under various operational conditions. The proposed model is designed in a MATLAB 2017 b environment.

Figure 12 shows the simulation diagram, which represents the power flow between the generating and load. The power has some variations in the grid or load side. It needs to be optimized by the reactive power control. A three-phase three-wire of VSI working either as UPQC with resilience random variance reduction technique (RRVR) controller is used for compensation. The above model can be tested under the dynamics load condition system.

Figure 13 represents the solar voltage generation; the above waveform clearly shows the output voltage $V = 510$ in the y-axis based on the time duration. For the stabilization purpose of wind energy generation, the proposed MPC is used. Due to this operation, a rectifier is utilized for AC to DC conversion. Figure 14 represents the rectified DC voltage of the wind energy generation, which is utilized for the MPC input source. The y-axis represents voltage; in $V = 450$ constant Voltage, the x-axis represents time $t = 1$ second.

Figure 14 demonstrates a fuel cell power generation based on two (voltage and current) waveforms. The fuel cell's voltage generation is 65 V, representing time in seconds from the above

figure's representation. Based on the voltage, the current value is 22 A with respect to time in seconds. The proposed RRVR based converter system continually produces power generation to the bus system because of utilizing the battery system. The battery-based energy management is operated in two modes of operation (i) charging mode (ii) Discharging mode. The above Fig. 14 shows the charging mode waveform of the battery system; the battery voltage is 440 V in the y-axis with one second time duration.

Figure 15 shows the active filter proposed in the THD survey using the RRVR algorithm; the output is gathered from the typical 4.85% THD and maintained with IEEE standard.

The system's dynamic load change will cause more voltage distortion, but it is clearly shown in Fig. 16 that the proposed RRVR will produce less voltage distortion during peak load conditions

Figure 17 shows the maximum amount of load change in implementing the UPQC model. 1500 Watts are used to analyze the proposed RRVR controller's performance, which is used to compensate for the load powerfully.

Figure 18 shows the stability analysis of the proposed UPQC model under dynamic load varying conditions. The 2000 W of the source (voltage and current) considerations are in phase with each other.

Figure 19 shows the result of using RRVR based THD method UPQC system. Based on this UPQC, RRVR produces 1.55% THD.
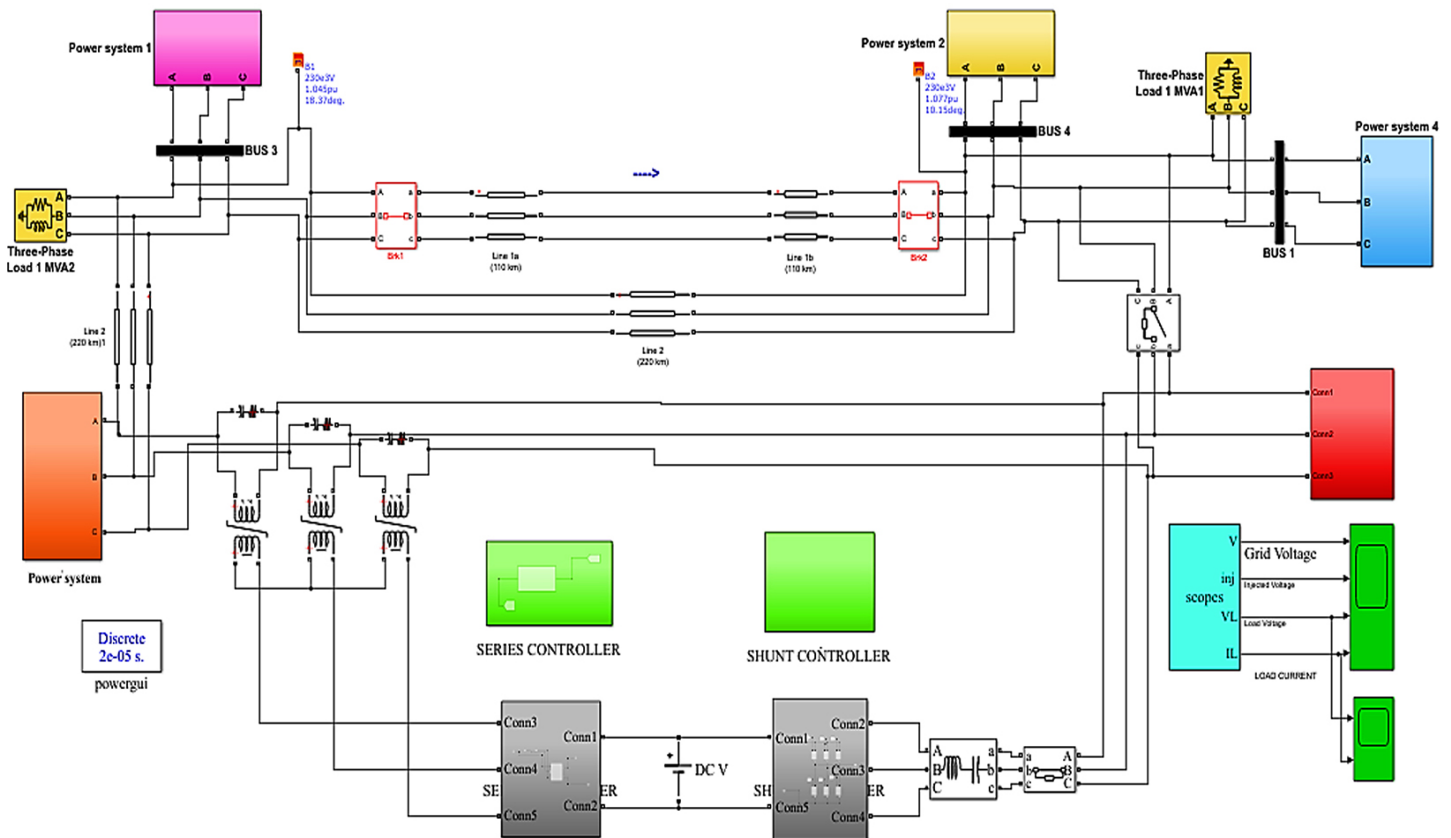


**Fig. 12.** Proposed simulation diagram of RRVR based UPQC model

8

Bull. Pol. Acad. Sci. Tech. Sci. 69(5) 2021, e137941

www.czasopisma.pan.pl          PAN          www.journals.pan.pl
POLSKA AKADEMIA NAUK

Design and analysis of the performance of multi-source interconnected electrical power system using resilience random variance reduction technique

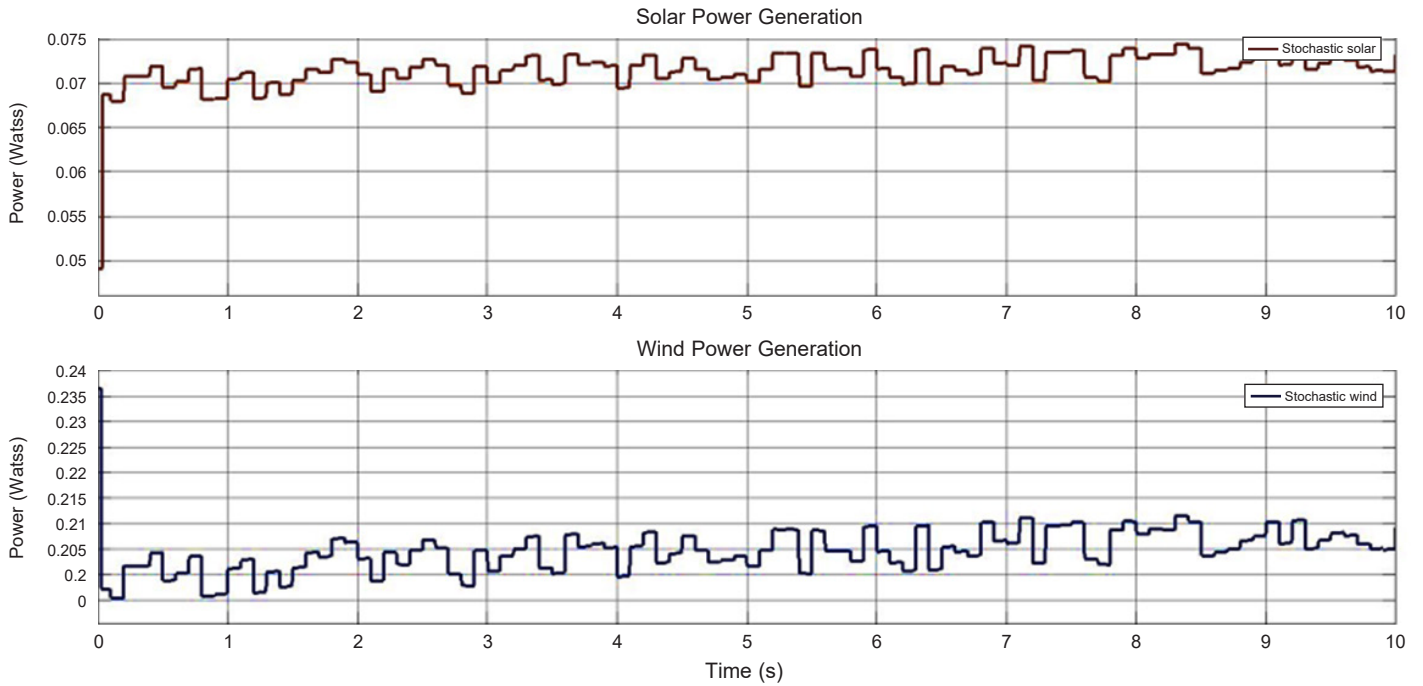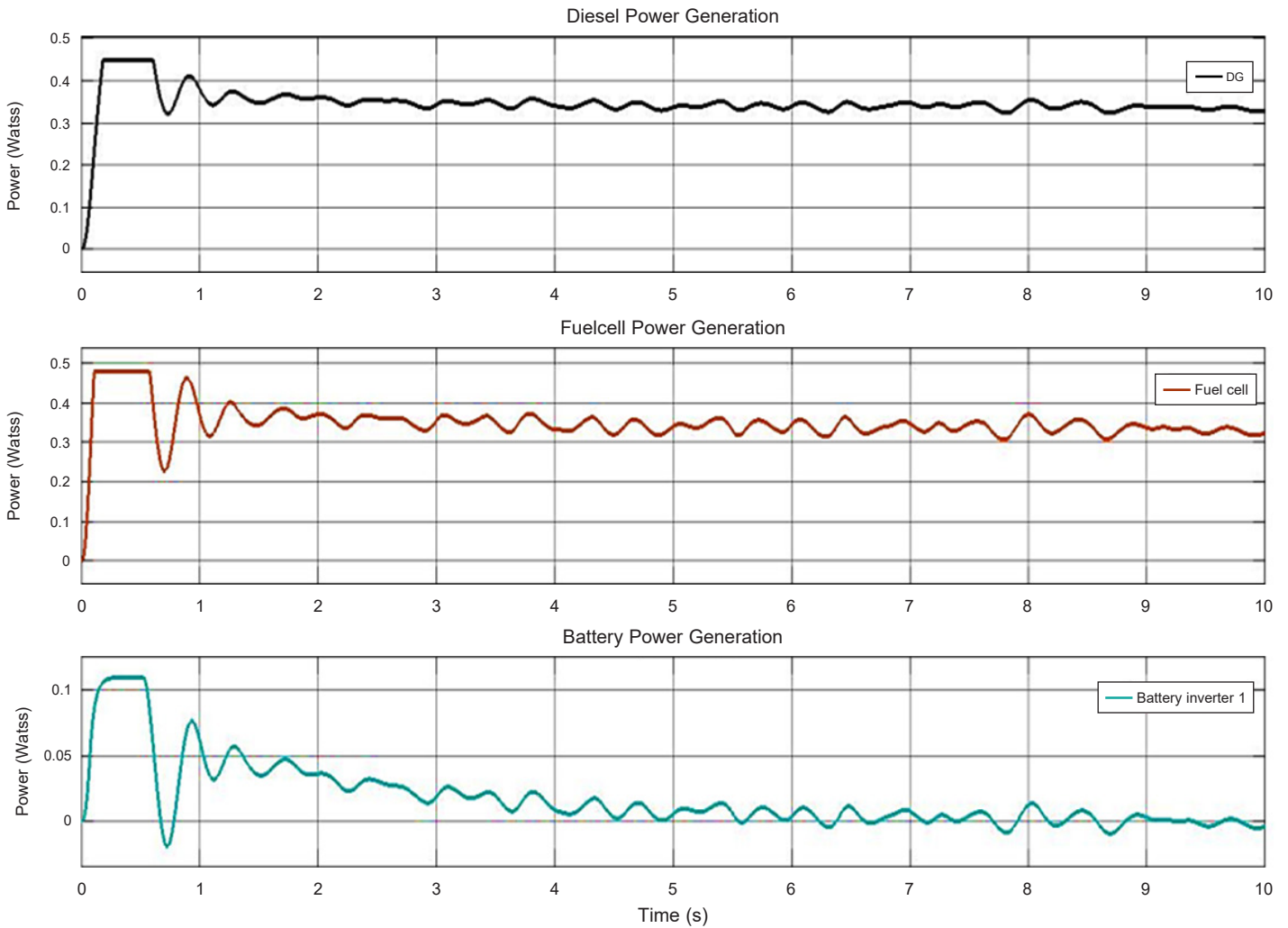**Fig. 13.** Solar voltage waveform
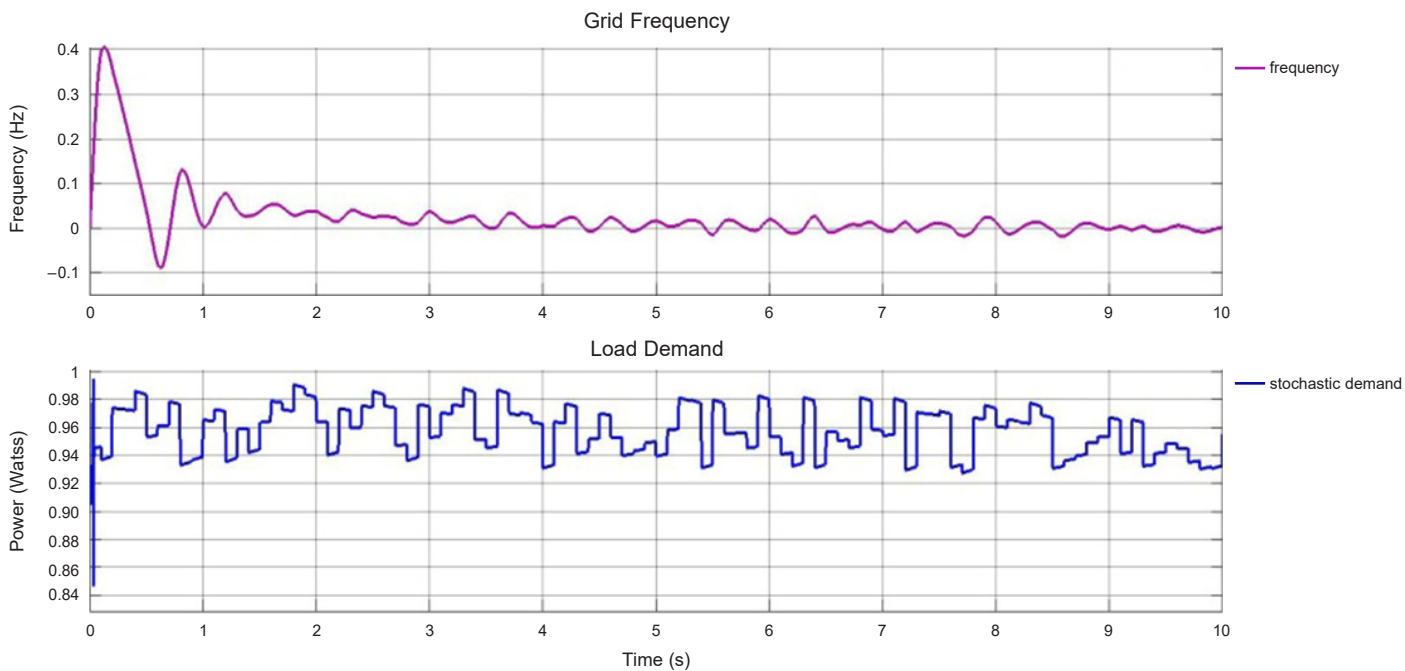


**Fig. 14.** Fuel Cell Generation Waveform

Bull. Pol. Acad. Sci. Tech. Sci. 69(5) 2021, e137941

9

B. Prakash Ayyappan and R. Kanimozhi



**Fig. 15.** Grid frequency with stochastic load demand
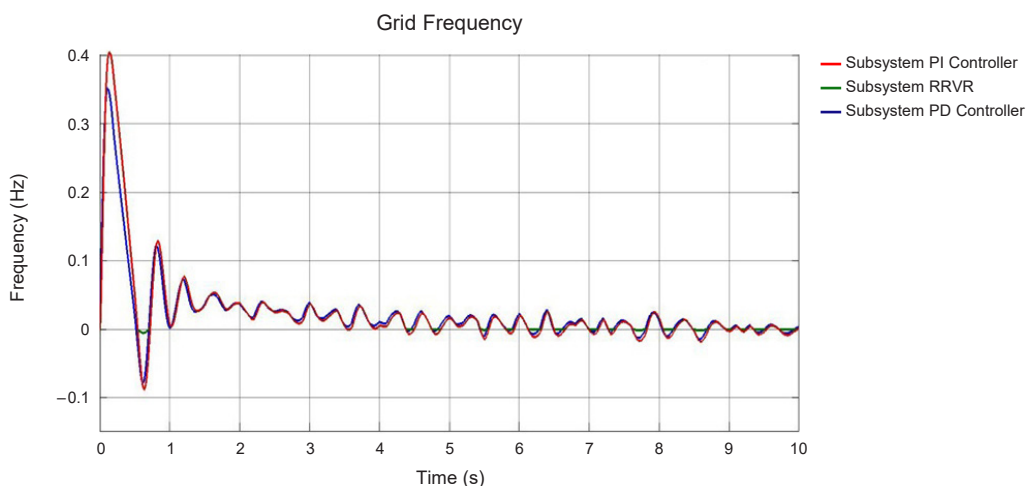


**Fig. 16.** Grid frequency with stochastic load demand


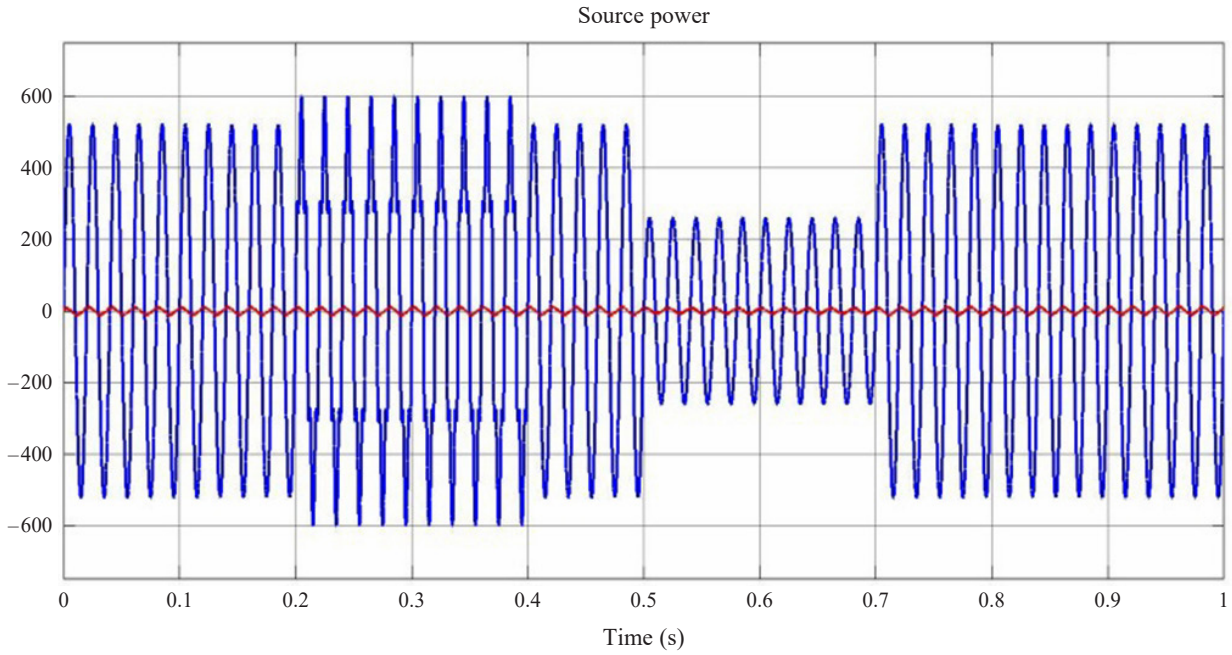
**Fig. 17.** Grid frequency with stochastic load demand

10

Bull. Pol. Acad. Sci. Tech. Sci. 69(5) 2021, e137941

Design and analysis of the performance of multi-source interconnected electrical power system using resilience random variance reduction technique
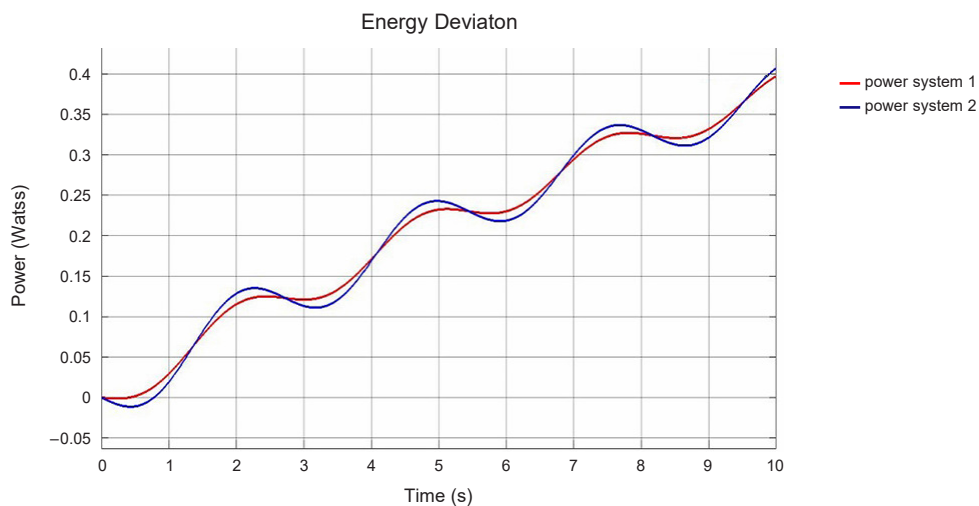
**Fig. 18.** Source power waveform for 2000 Watts
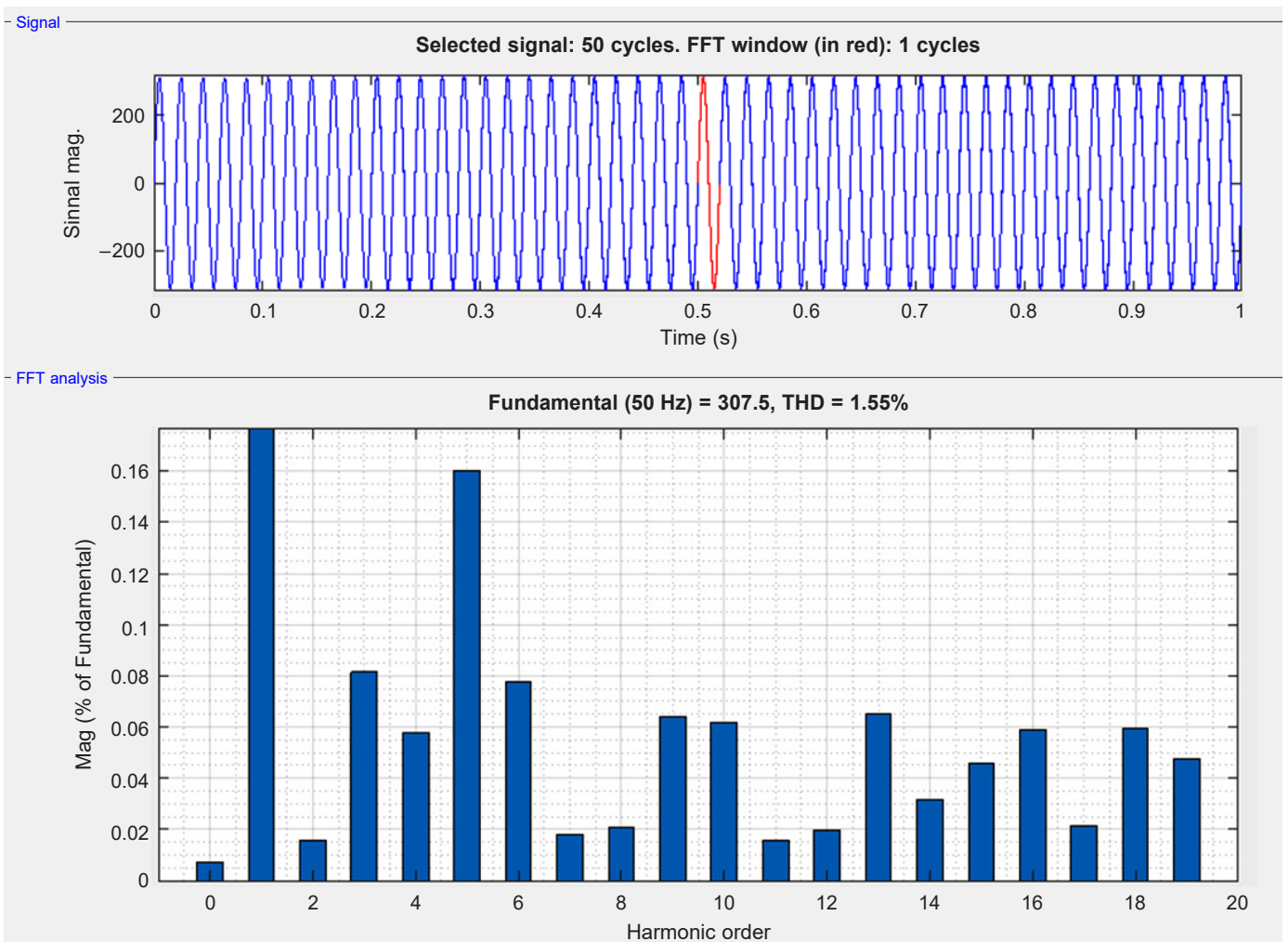
**Fig. 19.** THD exploration using RRVR technique

Bull. Pol. Acad. Sci. Tech. Sci. 69(5) 2021, e137941

11

**Tables 2**

Performance analysis of the proposed model without a controller

| S. No | Generating source power (W) | Generating source power (W) | | | Grid voltage (V) | Load voltage (V) | Grid frequency (Hz) |
|---|---|---|---|---|---|---|---|
| | | PV | WT | FC | | | |
| 1 | 500 | 200 | 150 | 150 | 300 | 310 | 48.9 |
| 2 | 1000 | 500 | 250 | 250 | 295 | 310 | 48.4 |
| 3 | 1500 | 600 | 500 | 400 | 288 | 310 | 47.6 |
| 4 | 2000 | 1000 | 600 | 400 | 280 | 310 | 47.1 |

| S. No | Power factor (%) | THD (%) | Sag voltage (V) | Swell voltage (V) | Steady-state error (%) | Settling time (s) |
|---|---|---|---|---|---|---|
| 1 | 0.986 | 5.9 | 140 | 340 | 2.6 | 0.4 |
| 2 | 0.982 | 6.4 | 155 | 355 | 3.1 | 0.46 |
| 3 | 0.972 | 7.1 | 165 | 365 | 3.4 | 0.49 |
| 4 | 0.968 | 8.6 | 160 | 360 | 3.9 | 0.51 |

**Tables 3**

Performance analysis of the proposed model with the controller

| S. No | Generating source power (W) | Generating source power (W) | | | Grid voltage (V) | Load voltage (V) | Grid frequency (Hz) |
|---|---|---|---|---|---|---|---|
| | | PV | WT | FC | | | |
| 1 | 500 | 200 | 150 | 150 | 300 | 299 | 48.9 |
| 2 | 1000 | 500 | 250 | 250 | 295 | 290 | 48.4 |
| 3 | 1500 | 600 | 500 | 400 | 288 | 285 | 48.1 |
| 4 | 2000 | 1000 | 600 | 400 | 280 | 275 | 47.8 |

| S. No | Power factor (%) | THD (%) | Sag voltage (V) | Swell voltage (V) | Steady-state error (%) | Settling time (s) |
|---|---|---|---|---|---|---|
| 1 | 0.996 | 1.5 | 140 | 340 | 0.7 | 0.28 |
| 2 | 0.991 | 1.8 | 155 | 345 | 1.1 | 0.32 |
| 3 | 0.990 | 1.9 | 155 | 345 | 1.3 | 0.39 |
| 4 | 0.989 | 2.1 | 150 | 340 | 1.7 | 0.41 |

Tables 2 demonstrate the proposed interconnected unified power quality conditioner (UPQC) without the controller table represented above. The proposed UPQC model does not produce stable power through the load system based on the above parameters.

Tables 3 describe the performance analysis of the proposed UPQC model with the RRVR controller. Based on the analysis of the various parameters like generating source power (W), grid voltage in (V), load voltage in (V), grid frequency in (Hz), power factor (%), THD (%), sag voltage(V), swell voltage(V), steady-state error (%), settling time (s), the proposed RRVR controller provide better result compared with without controller model.

Table 4 represents the performance analysis function of the UPQC using RRVR and existing systems with the PI-based controller on the above table, and the proposed RRVR techniques produce a better result.

Table 5 represents the load power stabilization of the proposed UPQC under different load variation system.

Figure 20 illustrates the load voltage and current stabilization system dynamic load power variation. The proposed RRVR

**Table 4**

Comparative analysis of the proposed UPQC using RRVR and existing PI controller in the systems

| Parameter | PI | RRVR |
|---|---|---|
| Steady-state error (%) | 1.8 | 0.7 |
| Settling time (s) | 0.46 | 0.28 |
| Without UPQC THD (%) | 18 | 7.96 |
| With UPQC THD (%) | 9.1 | 1.55 |
| Efficiency (%) | 88 | 93 |

**Table 5**

Load power stabilization for the proposed UPQC model

| Voltage (V) | Current (A) | Load (W) |
|---|---|---|
| 310 | 6.5 | 2000 |
| 310 | 5.0 | 1500 |
| 310 | 3.0 | 1000 |
| 310 | 1.5 | 500 |
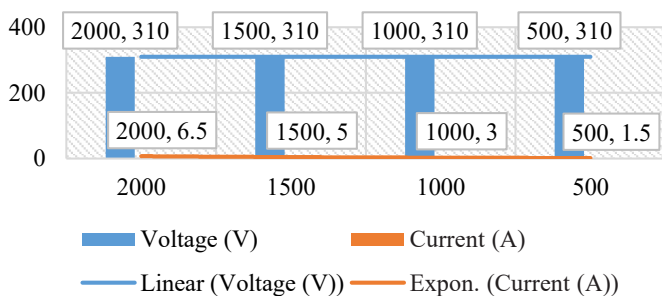
controller will remain in a stable load voltage load power of all changes.

Figure 21 is a comparative analysis of the steady-state error of the control UPQC and various parameters. Using PI to evaluate the efficiency and evaluation of THD results with or without UPQC compensator, the proposed RRVR can produce valid results.

Figure 22 is the THD for the proposed model, with the UPQC system producing a result of 1.55%, which is better than the existing model without UPQC.

Figure 23 represents the power factor graph for the maximum 2000 Watts load condition. During this state, the 0.995% power factor was achieved.

**Voltage and current variation for different loads**



**Fig. 20.** Voltage and current variation for different loads

12

Bull. Pol. Acad. Sci. Tech. Sci. 69(5) 2021, e137941

www.czasopisma.pan.pl    PAN    www.journals.pan.pl
POLSKA AKADEMIA NAUK

Design and analysis of the performance of multi-source interconnected electrical power system using resilience random variance reduction technique
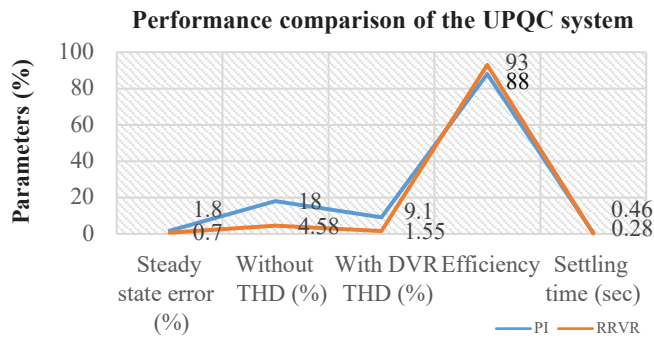
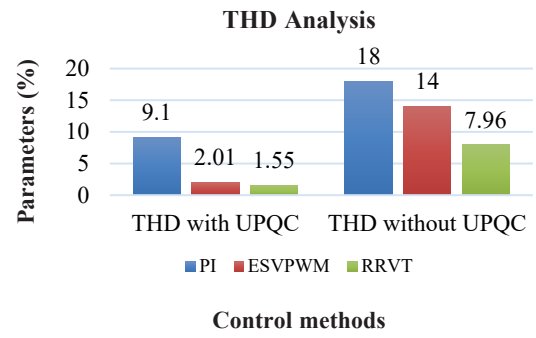**Fig. 21.** Performance analysis of the UPQC system
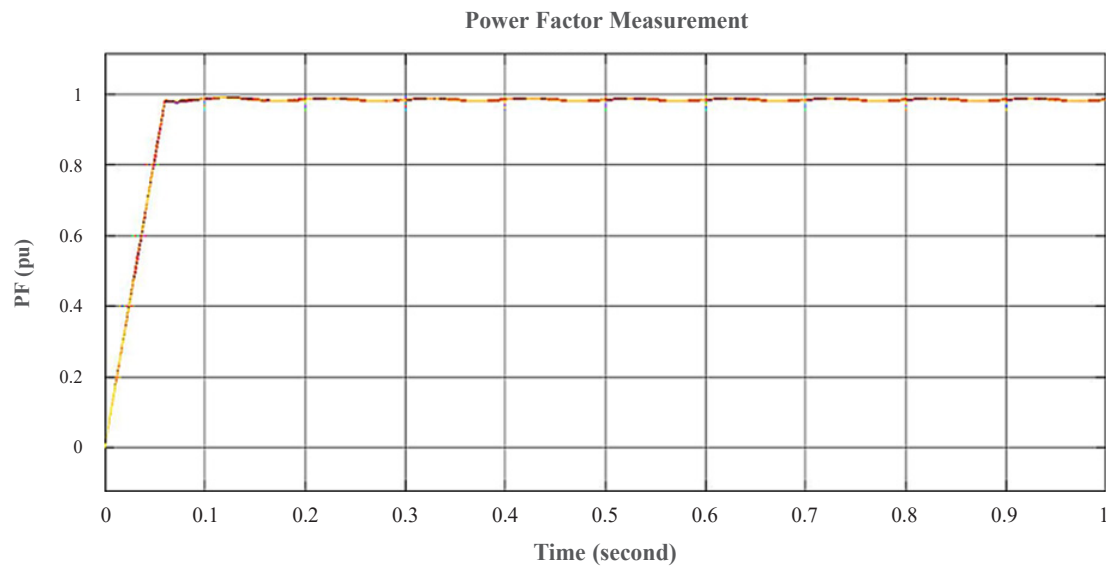


**Fig. 22.** THD Analysis



**Fig. 23.** Power factor graph

## 5. CONCLUSION

The performance of the implemented system has been validated under different load conditions. The proposed resilience random variance reduction technique (RRVR) has been used to reduce the loss and improve the system's stability like system voltage, current, frequency, settling time, power factor. The benefits of the proposed resilience random variance reduction technique were analyzed with different parameters like steady-state error (0.7%) of the system and the system's total harmonics distortion of 1.55% with UPQC. The result indicates that the coordinated UPQC and RRVR control technique will maintain the distribution system's optimal power flow. The purpose of the system's predictive power control is to control the reactive power in the UPQC to compensate for the grid voltage and current. With this new concept, the UPQC Compensators work efficiently and generate the required reactive power to optimize the grid power. Thus, the output voltage of the system will improve and meet the required load demand, and resilience random variance reduction technique (RRVR) has also been compared with PI-based controller in terms of steady-state error, settling time, total harmonic distortion and efficiency, and it provides an effective solution for the power quality stabilization problems.

## REFERENCE

[1] E. Sahin, "Design of an Optimized Fractional High Order Differential Feedback Controller for Load Frequency Control of a Multi-Area Multi-Source Power System With Nonlinearity," *IEEE Access*, vol. 8, pp. 12327–12342, 2020, doi: 10.1109/AC-CESS.2020.2966261.

[2] B. Zhao *et al.*, "Energy Management of Multiple Microgrids Based on a System of Systems Architecture," in *IEEE Trans. Power Syst.*, vol. 33, no. 6, pp. 6410–6421, Nov. 2018, doi: 10.1109/TPWRS.2018.2840055.

[3] M. Nilsson, L.H. Söder, and G.N. Ericsson, "Balancing Strategies Evaluation Framework Using Available Multi-Area Data," in *IEEE Trans. Power Syst.*, vol. 33, no. 2, pp. 1289–1298, March 2018, doi: 10.1109/TPWRS.2017.2736604.

[4] E. Tómasson and L. Söder, "Generation Adequacy Analysis of Multi-Area Power Systems With a High Share of Wind Power," in *IEEE Trans. Power Syst.*, vol. 33, no. 4, pp. 3854–3862, July 2018, doi: 10.1109/TPWRS.2017.2769840.

[5] B. Pan, W. Cong, M. Sun, J. Yu, and M. Zheng, "Fault location determination method for relay protection communication system based on power grid operation and maintenance multi-source data," *2019 IEEE Sustainable Power and Energy Conference (iSPEC)*, Beijing, China, 2019, pp. 2351–2356, doi: 10.1109/iSPEC48194.2019.8975178.

Bull. Pol. Acad. Sci. Tech. Sci. 69(5) 2021, e137941

13

B. Prakash Ayyappan and R. Kanimozhi

[6] G. Liu, M. Vrakopoulou and P. Mancarella, "Assessment of the capacity credit of renewables and storage in multi-area power systems," *IEEE Trans. Power Syst.*, doi: 10.1109/TP-WRS.2020.3034248.

[7] R. Patel *et al.*, "Enhancing Optimal Automatic Generation Control in a Multi-Area Power System With Diverse Energy Resources," *IEEE Trans. Power Syst.*, vol. 34, no. 5, pp. 3465–3475, Sept. 2019, doi: 10.1109/TPWRS.2019.2907614.

[8] H. Chen *et al.*, "Key Technologies for Integration of Multitype Renewable Energy Sources – Research on Multi-Timeframe Robust Scheduling/Dispatch," *IEEE Trans. Smart Grid*, vol. 7, no. 1, pp. 471–480, Jan. 2016, doi: 10.1109/TSG.2015.2388756.

[9] T.K. Mohapatra and B.K. Sahu, "Design and implementation of SSA based fractional order PID controller for automatic generation control of a multi-area, multi-source interconnected power system," *2018 Technologies for Smart-City Energy Security and Power (ICSESP)*, Bhubaneswar, 2018, pp. 1–6, doi: 10.1109/ICSESP.2018.8376697.

[10] C. Wang, K. Jia, B. Liu, and J. Zhang, "Coordination Control and Protection for Photovoltaic DC Distribution System," *2020 2nd International Conference on Smart Power & Internet Energy Systems (SPIES)*, Bangkok, Thailand, 2020, pp. 526–530, doi: 10.1109/SPIES48661.2020.9243132.

[11] H. Zhang, B. Zhang, A. Bose, and H. Sun, "A Distributed Multi-Control-Center Dynamic Power Flow Algorithm Based on Asynchronous Iteration Scheme," *IEEE Trans. Power Syst.*, vol. 33, no. 2, pp. 1716–1724, March 2018, doi: 10.1109/TPWRS.2017.2721405.

[12] A. Khoaei, M. Shahidehpour, L. Wu, and Z. Li, "Coordination of Short-Term Operation Constraints in Multi-Area Expansion Planning," *IEEE Trans. Power Syst.*, vol. 27, no. 4, pp. 2242–2250, Nov. 2012, doi: 10.1109/TPWRS.2012.2192507.

[13] D. Xu, J. Liu, X. Yan, and W. Yan, "A Novel Adaptive Neural Network Constrained Control for a Multi-Area Interconnected Power System With Hybrid Energy Storage," *IEEE Trans. Ind. Electron.*, vol. 65, no. 8, pp. 6625–6634, Aug. 2018, doi: 10.1109/TIE.2017.2767544.

[14] A. Nassaj and S.M. Shahrtash, "An Accelerated Preventive Agent-Based Scheme for Postdisturbance Voltage Control and Loss Reduction," *IEEE Trans. Power Syst.*, vol. 33, no. 4, pp. 4508–4518, July 2018, doi: 10.1109/TPWRS.2017.2778098.

[15] Y. Zhang, X. Liu,, and B. Qu, "Distributed model predictive load frequency control of multi-area power system with DFIGs," *IEEE/CAA J. Autom. Sin.*, vol. 4, no. 1, pp. 125–135, Jan. 2017, doi: 10.1109/JAS.2017.7510346.

[16] G. Tang, Z. Xu, H. Dong and Q. Xu, "Sliding Mode Robust Control Based Active-Power Modulation of Multi-Terminal HVDC Transmissions," *IEEE Trans. Power Syst.*, vol. 31, no. 2, pp. 1614–1623, March 2016, doi: 10.1109/TPWRS.2015.2429690.

[17] C. Zhong, J. Zhang, and Y. Zhou, "Adaptive Virtual Capacitor Control for MTDC System With Deloaded Wind Power Plants," IEEE Access, vol. 8, pp. 190582–190595, 2020, doi: 10.1109/ACCESS.2020.3032284.

[18] M. Kahl, C. Freye, and T. Leibfried, "A Cooperative Multi-Area Optimization With Renewable Generation and Storage Devices," *IEEE Trans. Power Syst.*, vol. 30, no. 5, pp. 2386–2395, Sept. 2015, doi: 10.1109/TPWRS.2014.2363762.

[19] J. Zhao *et al.*, "A Multi-Source Coordinated Optimal Operation Model Considering the Risk of Nuclear Power Peak Shaving and Wind Power Consumption," *IEEE Access*, vol. 8, pp. 189702–189719, 2020, doi: 10.1109/ACCESS.2020.3027705.

[20] W. Wang, L. Jiang, Y. Cao, and Y. Li, "A Parameter Alternating VSG Controller of VSC-MTDC Systems for Low-Frequency Oscillation Damping," *IEEE Trans. Power Syst.*, vol. 35, no. 6, pp. 4609–4621, Nov. 2020, doi: 10.1109/TPWRS.2020.2997859.

[21] T. Yang, S. Bozhko, J. Le-Peuvedic, G. Asher, and C.I. Hill, "Dynamic Phasor Modeling of Multi-Generator Variable Frequency Electrical Power Systems," *IEEE Trans. Power Syst.*, vol. 31, no. 1, pp. 563–571, Jan. 2016, doi: 10.1109/TP-WRS.2015.2399371.

[22] P.M. Dash, S.K. Mohapatra, and A.K. Baliarsingh, "Tuning of LFC in Multi-source Electrical Power Systems Implementing Novel Nature-Inspired MFO Algorithm Based Controller Parameter," *2020 International Conference on Computational Intelligence for Smart Power System and Sustainable Energy (CISPSSE)*, Keonjhar, Odisha, India, 2020, pp. 1–5, doi: 10.1109/CISPSSE49931.2020.9212199.

[23] F. Qi, M. Shahidehpour, F. Wen, Z. Li, Y. He, and M. Yan, "Decentralized Privacy-Preserving Operation of Multi-Area Integrated Electricity and Natural Gas Systems With Renewable Energy Resources," *IEEE Trans. Sustainable Energy*, vol. 11, no. 3, pp. 1785–1796, July 2020, doi: 10.1109/TSTE.2019.2940624.

[24] X.S. Zhang, T. Yu, Z.N. Pan, B. Yang, and T. Bao, "Lifelong Learning for Complementary Generation Control of Interconnected Power Grids With High-Penetration Renewables and EVs," *IEEE Trans. Power Syst.*, vol. 33, no. 4, pp. 4097–4110, July 2018, doi: 10.1109/TPWRS.2017.2767318.

[25] A. Khanjanzadeh, S. Soleymani, and B. Mozafari, "A decentralized control strategy to bring back frequency and share reactive power in isolated microgrids with virtual power plant," *Bull. Pol. Acad. Sci. Tech. Sci.*, vol. 69, No. 1, pp. 1–9, 2021, doi: 10.24425/bpasts.2021.136190.

[26] M. Parol and M. Polecki, "The performance of passive methods of detecting island operation implemented in PV inverters during selected disturbances in distribution power grids," *Bull. Pol. Acad. Sci. Tech. Sci.*, vol. 68, no. 5, pp. 1087–1098, 2020. doi: 10.24425/bpasts.2020.134658.

[27] A. Bobori, S. Paszek, A. Nocori, and P. Pruski, "Determination of synchronous generator nonlinear model parameters based on power rejection tests using a gradient optimization algorithm," *Bull. Pol. Acad. Sci. Tech. Sci.*, vol. 65, no. 4, pp. 479–488, 2017, doi: 10.1515/bpasts-2017-0053.

[28] G. Benysek, "Improvement in the efficiency of the distributed power systems," *Bull. Pol. Acad. Sci. Tech. Sci.*, vol. 57, no. 4, pp. 369–374, 2009, doi: 10.2478/v10175-010-0140-1.

[29] H. Rezk, M.A. Mohamed, A.A. Zaki Diab, and N. Kanagaraj, "Load Frequency control of Multi-interconnected Renewable Energy Plants using Multi-Verse Optimizer," *Comput. Syst. Sci. Eng.*, vol. 37, no. 2, pp. 219–231, 2021, doi: 10.32604/csse.2021.015543.

[30] H. Sun, C. Peng, D. Yue, Y.L. Wang, and T. Zhang, "Resilient Load Frequency Control of Cyber-Physical Power Systems Under QoS-Dependent Event-Triggered Communication," IEEE Trans. Syst. Man Cybern.: Syst., vol. 51, no. 4, pp. 2113–2122, doi: 10.1109/TSMC.2020.2979992.

[31] E. Canelas, T. Pinto-Varela, and B. Sawik, "Electricity Portfolio Optimization for Large Consumers: Iberian Electricity Market Case Study," *Energies*, vol. 13, no. 9, p. 2249, 2020, doi: 10.3390/en13092249.